Desalination and Water Treatment
www.deswater.com

doi: 10.5004/dwt.2023.29997

311 (2023) 228–236
November

Highly selective and efficient removal of phosphate by $La(OH)_3$-loaded *Juncus effusus* with a three-dimensional structure

Yuhang Xu, Wei Li, Sisi Qin, Kai Su, Junmin Chen*, Shengli Zhang*

Faculty of Geosciences and Environmental Engineering, Southwest Jiaotong University, 611756 Chengdu, Sichuan, China, emails: cjm@swjtu.edu.cn (J. Chen); zhang222@home.swjtu.edu.cn (S. Zhang)

Received 30 July 2023; Accepted 22 September 2023

ABSTRACT

In this study, $La(OH)_3$-loaded *Juncus effusus* (La-JE) with a three-dimensional structure was prepared via an *in-situ* precipitation and then wrapped in a cellulose membrane. The La-JE not only avoided the leakage of $La(OH)_3$ but also was separated from solution easily. The optimal pH for phosphate removal by the La-JE was 6. The removal rate of phosphate was positively correlated with adsorption time, La-JE dosage and reaction temperature, and negatively correlated with phosphate concentration. The adsorption process conformed to pseudo-second-order kinetic model and was better fit by Freundlich model. At 25°C, the maximum adsorption capacity of the La-JE was 22.75 mg·P/g. The influence of SO_4^{2-}, Cl^-, NO_3^-, NH_4^+, HCO_3^- and CO_3^{2-} on phosphate removal was negligible, suggesting that the La-JE had good anti-interference ability. Mechanism analysis showed that the removal process of phosphate was related to both ligand exchange and surface precipitation. The application in real water environment exhibited that the La-JE had good potential for advanced dephosphorization of sewage treatment plant and natural waterbody remediation.

Keywords: Adsorption; Lanthanum hydroxide; Phosphate; *Juncus effusus*; Cellulose

1. Introduction

Phosphorus (P) is essential for the growth of animals and plants. However, due to excessive release of phosphorus in the rivers or lakes, about 30%–50% of water sources are facing the eutrophication [1]. Eutrophication of the water bodies could destruct water ecosystems and threaten human health [2]. The minimum margin concentration of phosphate to induce eutrophication is 0.02 mg/L [3]. Therefore, the effective removal of phosphate has become an urgent issue for the protection of natural waters.

Various methods including biological treatment, chemical precipitation, ions exchange, membrane process and adsorption, have been employed to reduce phosphorus in water and wastewater [4–7]. However, biological treatment and chemical precipitation are not applicable to the removal of low-concentration phosphate, while ion exchange and membrane process need high technological equipment and operation costs [8,9]. By contrast, adsorption method has the appealing advantages of simple operation, high efficiency, cost-effective and low sludge production [10,11].

Many adsorbents like metal oxide and metal hydroxide [12], bentonite [13], activated carbon [14] and metal–organic frameworks [15] have been reported. In particular, Lanthanum (La)-containing absorbents stand out due to their high affinity for phosphate and low solubility constant (pKsp = 26.15) of the formed lanthanum phosphate in a relatively acidic environment [16,17]. However, the reported La-containing active species commonly had a nanostructure, which are not only easy to agglomerate but also difficult to separate from aqueous solution [18]. In addition, the leakage of nanoparticles into water will pose great challenge in practice [19]. Hence, some studies have tried

* Corresponding author.

to load nano-lanthanum oxide or hydroxide on different matrixes such as magnetic particles, carbon materials and polymers [20–22].

Juncus effusus (JE) is a type of natural cellulose that is extensively cultivated in various regions of China. One of its unique characteristics is the three-dimensional (3D) network structure, which consists of interconnected channels, being a promising polymer carrier [23]. However, due to the strong hydrophobicity of JE fibers, the introduction of active groups is obstructed. Our previous work demonstrated that its hydrophobicity can be overcome by means of ethanol/aqueous solution [24]. Herein, La^{3+} was rapidly introduced into the 3D structure of the JE in ethanol/water system and then transformed into $La(OH)_3$ in situ via reacting with ammonia in the present study. Afterward, a layer of cellulose film was coated outside of the JE to obtain the $La(OH)_3$-loaded *Juncus effusus* (La-JE). The morphology and structure of the La-JE were characterized by scanning electron microscopy (SEM), X-ray diffraction (XRD) and Fourier-transform infrared spectroscopy (FTIR). Batch experiments were done for investigating the adsorption potential of the La-JE for phosphate. At the same time, the anti-interference ability and reusability of the La-JE were assessed, and the adsorption mechanism was elucidated.

2. Materials and methods

2.1. Materials

JE was obtained from Guangxi Golden rabbit Ecological Agriculture Co., Ltd., China. $LaCl_3{\cdot}7H_2O$, ammonium molybdate and ascorbic acid were bought from Aladdin Biochemical Technology Co., Ltd., China. Ammonia, ethanol, KH_2PO_4, HCl and NaOH were provided by Chengdu Kelong Chemicals Co., Ltd., China. All reagents were AR grade.

2.2. Preparation and characterization of the La-JE

The preparation of La-JE was done according to the procedure presented in Fig. 1. Briefly, 0.2 g of JE was immersed in 50 mL of 20 g/L $LaCl_3$ ethanol/water solution with 1:1 for ethanol and water volume ratio. After 10 min, the JE was transferred onto a polyethylene (PE) web. When the surface moisture was dried out, the sample was put in an ammonia ethanol/water solution with 1:3 for ammonia and ethanol/water volume ratio and 1:1 for ethanol and water volume ratio for 60 min. Subsequently, it was transferred onto the PE web again for drying out the surface moisture. Later, the material was soaked in a 2% cellulose solution for 5 s, and then it underwent a process of regeneration in deionized water. The resulting sample was labelled as La-JE.

The physical morphologies, crystal structure and functional groups of the samples including JE, La-JE and P-loaded La-JE were characterized by JSM-7001F SEM (Japan), Bruker D8 XRD (Germany) analysis and Nicolet iS50 Infrared Spectrometer , America (FTIR), respectively.

2.3. Batch adsorption experiments

La-JE (0.4–3.6 g/L) was dispersed in 50 mL phosphate working solution of known concentrations (10–50 mg·P/L) at various pH 2–10. The mixture was shaken for different time (5 min–6 h) at the predetermined temperature (15°C–45°C). For each experiment, the residual concentrations of phosphate in the aqueous samples were quantified by molybdenum blue spectrophotometric analysis. The percentage of phosphate removal (%) and the adsorption capacity (mg·P/g) of the La-JE were computed using Eqs. (1) and (2), respectively.

$$\eta = \frac{C_0 - C_e}{C_0} \times 100\% \tag{1}$$

$$q = \frac{\left(C_0 - C_t\right) \times V}{m} \tag{2}$$

where C_0, C_e and C_t are the phosphate concentrations at initial, equilibrium and time t, respectively, and their units are

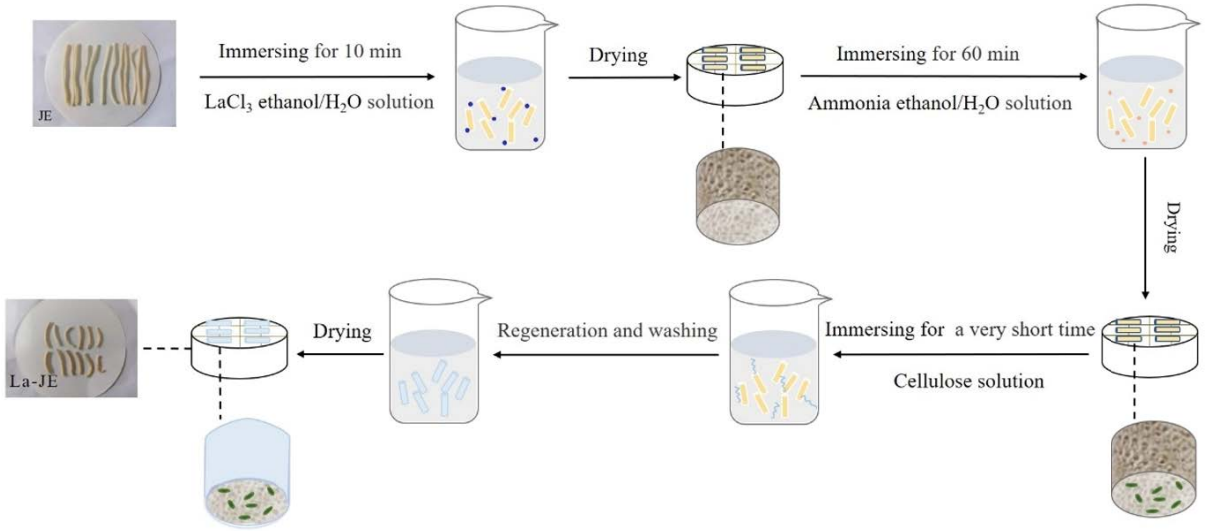

Fig. 1. Synthetic scheme for the preparation of the La-JE.

mg/L; *m* is the La-JE mass (g), and *V* is the volume of phosphate solution (L).

2.4. Influence of coexisting ions and regeneration experiment

SO_4^{2-}, Cl^-, NO_3^-, NH_4^+, HCO_3^- and CO_3^{2-} were chosen as the coexisting ions for assessing the anti-interference ability of the La-JE. The concentration of phosphate and each coexisting ion were set at 10 mg·P/L and 250 mg/L, respectively.

Reusable study was performed by suspending 0.05 g of La-JE in 10 mg·P/L of phosphate solution at 25°C. When adsorption equilibrium was reached, the P-loaded La-JE was desorbed using 1 mol/L NaOH solution. Afterward, it was reused in the next cycle.

3. Results and discussion

3.1. Characterization of the samples

The cross-section morphologies of the JE and La-JE are displayed in Fig. 2. It was clear that the JE had a 3D network structure, and its surface was relatively smooth. When $La(OH)_3$ was loaded, the 3D structure was completely preserved and the JE fiber was coated by many lamellas. At the same time, the regenerated cellulose was observed to form a dense film on the La-JE surface, which can prevent the leakage of La-containing species.

The XRD patterns of the JE and La-JE are shown in Fig. 3a. Compared with the JE, some new diffraction peaks appeared at 15.6°, 27.2°, 28.0°, 39.4° and 48.6° for the La-JE, which proved that the La-containing species loaded on the JE were $La(OH)_3$.

The FTIR spectra of the JE, La-JE and P-loaded La-JE are shown in Fig. 3b. The new peaks appearing at 3,445 and 670 cm^{-1} in the FTIR spectrum of the La-JE belonged to the La-OH vibration of $La(OH)_3$ [25,26]. Due to the existence of a large amount of hydroxyl group, the adsorption band at 3,340 cm^{-1} gave a red shift and became stronger. These further confirmed to the successful introduction of $La(OH)_3$. As for the disappeared adsorption peaks at 1,600 and 1,510 cm^{-1}, it was related to the lignin removal on the JE during soaking in ammonia ethanol/water.

3.2. Effect of initial pH

For phosphate adsorption on the La-JE, pH is the most important factor. Hence, the influence of solution pH (2–10) on phosphate adsorption was done by dispersing La-JE (2 g/L) in a phosphate solution (10 mg·P/L) and shaking for 240 min at 25°C. From the result shown in Fig. 4a it is clear that with solution pH rising from 1.8 to 9.8, phosphate removal rate firstly gave an increase and then decreased. The optimal pH was found to be 6. The reason is that phosphate exists different species including H_3PO_4, $H_2PO_4^-$, HPO_4^{2-} and PO_4^{3-} with solution pH varying [27,28]. When pH is below 2.1, the form of relatively stable H_3PO_4 dominates, but the interaction between H_3PO_4 and the adsorbent is weak. With pH increases from 2.1 to 12.3, $H_2PO_4^-$ and HPO_4^{2-} became the main species in turn. Because the adsorption free energy of $H_2PO_4^-$ was lower, its adsorption on the adsorbent was easier than HPO_4^{2-} [28]. After that, PO_4^{3-} becomes the major specie. In addition, the decline of phosphate removal rate in strong acid condition was related to the leaking of lanthanum ions. According to Chen et al. [29], a significant leaking of La (>60%) was observed under the condition of pH 3.0, but the leaking of La was negligible with pH ≥ 4.0. Under strong alkaline condition, the decreased percentage was also ascribed to the inhibitory effect of OH^- on the formation of $LaPO_4$ [30].

3.3. Effect of adsorption time

Influence of adsorption time (5 min–6 h) on phosphate removal was carried out via dispersing La-JE (2 g/L, pH = 6) in a phosphate solution (10 mg·P/L) and shaking

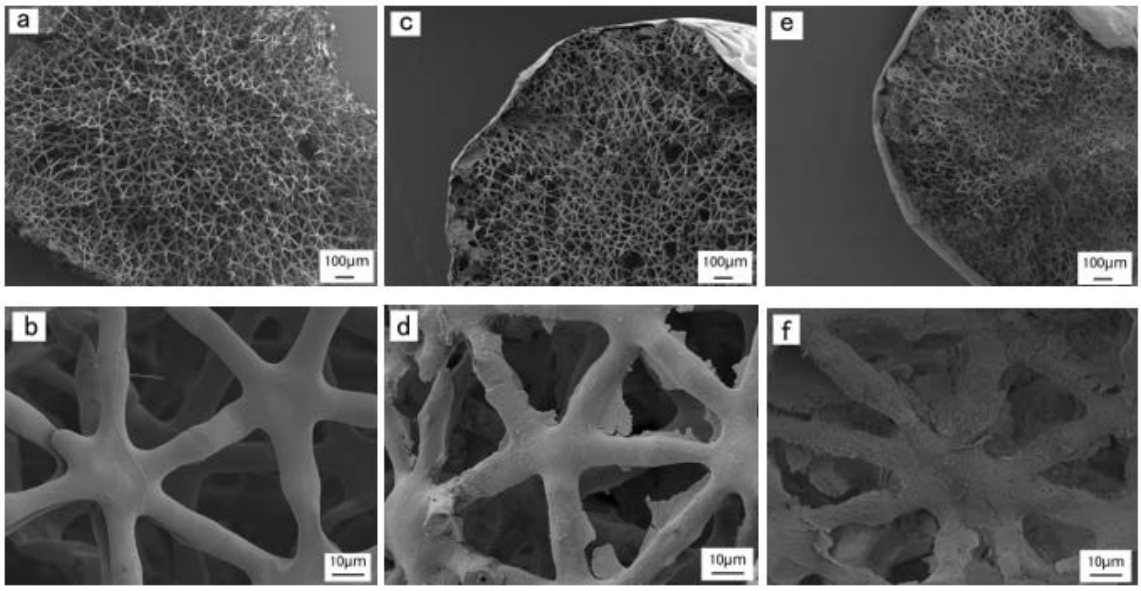

Fig. 2. Scanning electron microscopy images of the JE (a,b), La-JE (c,d) and P-loaded La-JE (e,f) cross-section.

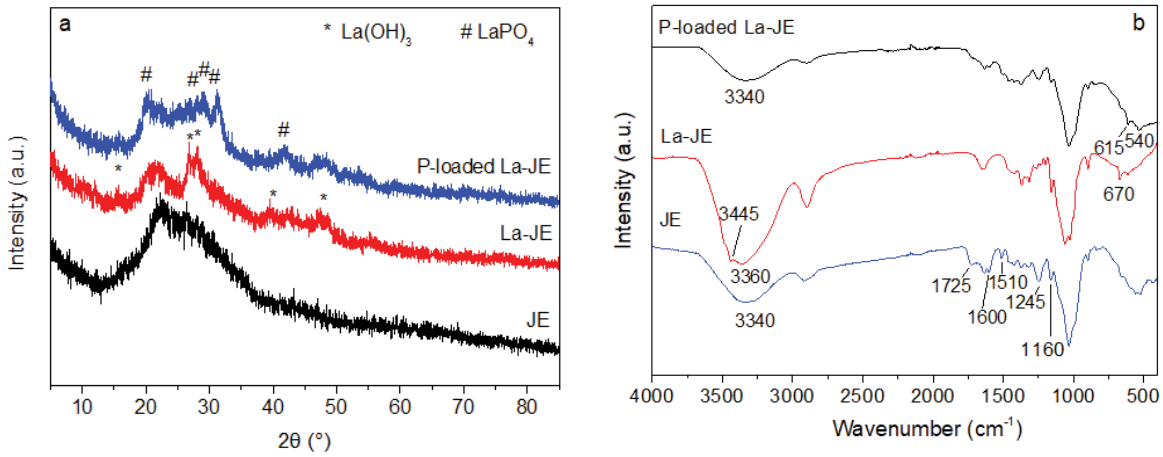

Fig. 3. X-ray diffraction patterns (a) and Fourier-transform infrared spectra (b) of the JE, La-JE and P-loaded La-JE.

for 240 min at 25°C. The result is displayed in Fig. 4b. It is evident that the removal rate of phosphate rapidly rose at the initial stage of adsorption (5–30 min). Then, the increment gradually decreased and reached the adsorption equilibrium after 180 min. It is due to the fact that there existed more adsorption sites on the La-JE for phosphate binding at the beginning stage. In addition, the higher concentration gradient also caused the stronger adsorption force. While the reaction time was prolonged, the adsorption potential decreased because of the fewer adsorption sites and lower phosphate concentration. Accordingly, the adsorption rate also decreased. Finally, the adsorption–desorption equilibrium was reached.

3.4. Effect of La-JE dosage

By dispersing La-JE (2 g/L) in a phosphate solution (10 mg·P/L, pH = 6) and shaking for 240 min at 25°C, the effect of La-JE dosage (0.4–3.6 g/L) on phosphate removal was performed. The result is presented in Fig. 4c. As the dosage of La-JE increased from 0.4 to 3.6 g/L, the removal rate of phosphate steadily rose from 59% to 99%. Meanwhile, the adsorption capacity of the La-JE gradually reduced from 14.8 to 2.7 mg/g. The phenomenon was because increasing the dosage of La-JE, the available active sites increased. Thus, more phosphate can be adsorbed by the La-JE, improving the removal rate. However, more adsorption sites were not effectively utilized due to the fixed phosphate concentration, so the adsorption capacity dropped. Considering the removal rate and economy, the La-JE dosage was fixed 2 g/L in subsequent experiments.

3.5. Effect of initial phosphate concentration

With dispersing La-JE (2 g/L) in a phosphate solution (pH = 6) and shaking for 240 min at 25°C, the effect of initial phosphate concentration (10–50 mg·P/L) was investigated. The result was shown in Fig. 4d. With phosphate concentration varying from 10 to 50 mg/L, the removal rate decreased from 93% to 75%. At the same time, the adsorption capacity of the La-JE increased from 4.6 to 18.9 mg/g. The reason is that when the initial phosphate concentration was low, almost all of phosphate was adsorbed by the La-JE, so the removal rate was high. However, because of the too low phosphate concentration, some active sites on the La-JE were still in idle state, causing that the adsorption capacity was relatively low. As the phosphate concentration increased, the idle adsorption sites were gradually occupied, and the adsorption capacity also increased.

3.6. Effect of reaction temperature

By dispersing 2 g/L La-JE in a phosphate solution with 10 mg·P/L, solution pH = 6 and reaction time of 240 min, the influence of reaction temperature (15°C–45°C) on phosphate removal was studied. It was obvious from Fig. 4e that when reaction temperature rose from 15°C to 45°C, the removal rate of phosphate increased from 91.56% to 98.37%, and the adsorption capacities increased from 4.5 to 4.9 mg/g. However, the increment was small, suggesting that the influence of reaction temperature on phosphate removal was slight.

3.7. Adsorption kinetics

To study the potential rate controlling step and adsorption mechanism, pseudo-first-order and pseudo-second-order kinetic equations were employed to analyze the kinetic data, respectively. The fitting results are provided in Fig. 5 and Table 1.

It is obvious that the pseudo-second-order kinetic model had the higher R^2 values ($R^2 > 0.99$) than the pseudo-first-order kinetic model. Moreover, the adsorption capacities ($q_{e,cal}$) calculated by the former were also closed to the experimental results ($q_{e,exp}$). So, the phosphate adsorption on the La-JE complied with the pseudo-second-order kinetic model, suggesting that the adsorption process was mainly chemisorption.

3.8. Adsorption isotherms

To evaluate the adsorption performance of the La-JE for phosphate, the adsorption equilibrium data were analyzed by Langmuir and Freundlich isotherm models, respectively. The fitting curves are demonstrated in Fig. 6, and the corresponding parameters are listed in Table 2.

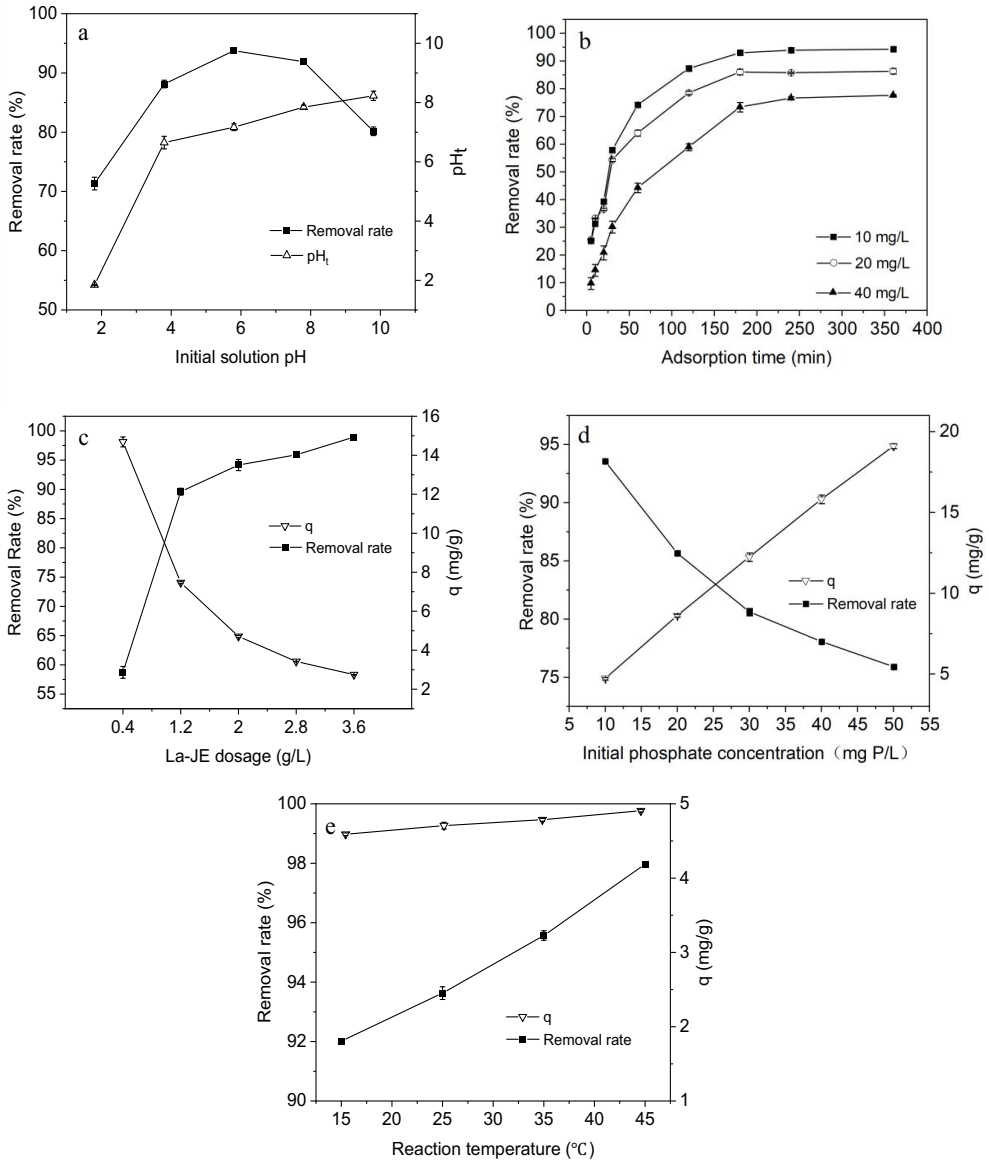

Fig. 4. Effects of initial solution pH (a), adsorption time (b), La-JE dosage (c), initial phosphate concentration (d) and reaction temperature (e) on phosphate removal.

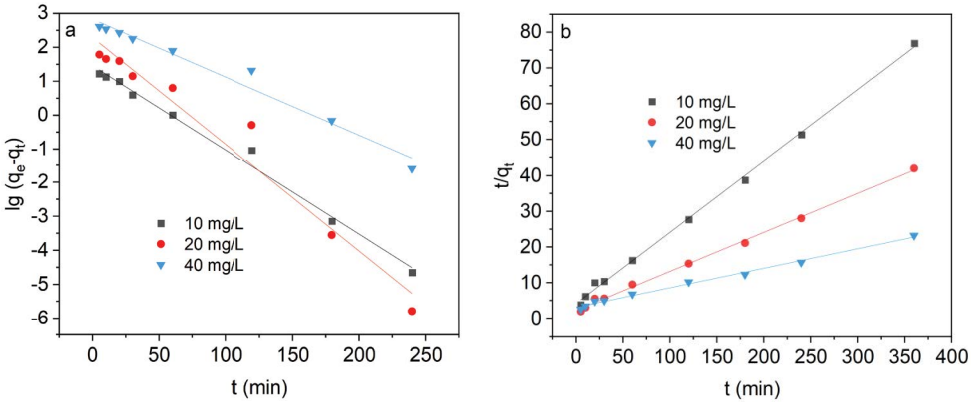

Fig. 5. Pseudo-first-order (a) and pseudo-second-order (b) kinetic models for phosphate adsorption on the La-JE.

Table 1
Parameters of two kinetic models for phosphate adsorption on the La-JE

		Pseudo-first-order kinetic			Pseudo-second-order kinetic		
C_0 (mg/L)	$q_{e,exp}$ (mg/g)	$q_{e,cal}$ (mg/g)	k_1 (min^{-1})	R^2	$q_{e,cal}$ (mg/g)	k_2 (g/mg·min)	R^2
10	4.68	4.28	0.0248	0.9892	5.02	0.0094	0.9979
20	8.56	9.84	0.0314	0.9548	9.15	0.0053	0.9972
40	15.53	16.90	0.0171	0.9671	18.28	0.0010	0.9922

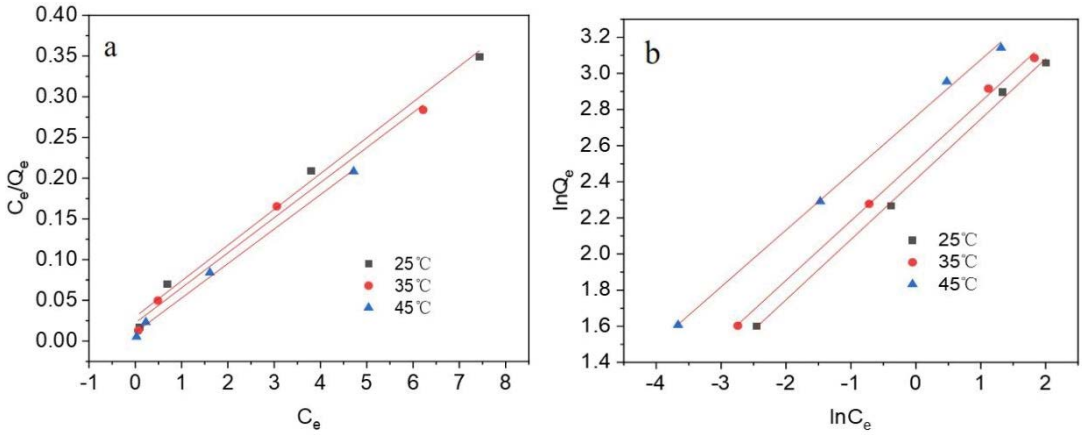

Fig. 6. Langmuir (a) and Freundlich (b) isotherms for phosphate adsorption on the La-JE.

Table 2
Fitting parameters of two adsorption isotherms at different temperatures

T (°C)	Langmuir isotherm model			Freundlich isotherm model		
	Q_m (mg/g)	K_L (L/mg)	R^2	K_F ($mg^{1-1/n}\cdot L^{1/n}\cdot g^{-1}$)	n	R^2
25	22.75	1.4728	0.9865	11.1766	2.9991	0.9972
35	23.21	1.9339	0.9880	12.3507	3.0340	0.9976
45	23.60	4.0574	0.9951	15.8259	3.1810	0.9969

The results demonstrate that two models had a good correlation with the equilibrium data. However, the R^2 values obtained by the Freundlich model were slightly greater (>0.99) than that of the Langmuir model, suggesting that the phosphate adsorption on the La-JE was more consistent with the Freundlich model. Similar result was reported for phosphorus adsorption on the La(III) loaded granular ceramic [31]. In addition, $n > 1$ displayed that the La-JE had a good affinity for phosphate. At 25°C, 35°C and 45°C, the La-JE displayed the maximum adsorption capacities of 22.75, 23.21 and 23.60 mg/g, respectively. It was not as high as that of some La-loaded powdered sorbents (Table 3), but had a macroscopic size and was easily separated from aqueous solution.

Table 3
Comparison of the adsorption capacities of the La-JE and other La-loaded adsorbents for phosphate

Adsorbent	T (°C)	Q_{max} (mg/g)	References
Phoslock®	35	10.5	[17]
La-BC	25	31.94	[20]
Mag-MSNs-42%La	30	54.2	[29]
PVA-SA-LH	25	7.89	[32]
NT-25 La	25	14.0	[33]
La-JE	25	22.75	This work

3.9. Thermodynamic study

To further comprehend the adsorption mechanism, three thermodynamic parameters (ΔG, ΔH, ΔS) were computed according to the van't Hoff equation.

From the results listed in Table 4, it can be seen that all of the calculated $\Delta G°$ were negative, which revealed the spontaneity of the phosphate adsorption on the La-JE. The positive $\Delta H°$ confirmed the endothermic nature of adsorption, which was consistent with the result obtained from Fig. 2e. The positive $\Delta S°$ suggested that the disorder at

the solid/solution interface increased with the progress of the adsorption reaction.

3.10. Anti-interference ability and reusability of the La-JE

The effects of coexisting ions including SO_4^{2-}, Cl^-, NO_3^-, NH_4^+, HCO_3^- and CO_3^{2-} on phosphate adsorption on the La-JE were investigated. According to the results shown in Fig. 7a, the fluctuation range of phosphate removal rate was only ±4% compared with the absence of coexisting ion. Hence, the coexistence of SO_4^{2-}, Cl^-, NO_3^-, NH_4^+, HCO_3^- and CO_3^{2-} had no significant influence on the phosphate adsorption, indicating that the La-JE had good anti-interference ability. In contrast, the presence of CO_3^{2-} exerted a negative influence on phosphate removal in quite a few literatures [34–36].

To study the reusability of the La-JE, the desorption experiment was done. Compared with the first adsorption, the removal rate of phosphate sharply reduced from 93.48% to 70.19% for the second adsorption, and then to 44.12% for the third adsorption. In the fourth cycle, the removal rate only reduced by 0.77%. This meant that the P loaded on the La-JE was not completely reversible. The similar conclusions have been reported by Chen et al. [31] and Yao et al. [37]. The reason was attributed to the different interactions between La-loaded adsorbents and P-containing species. When ion exchange and electrostatic attraction are the main mechanisms of phosphate adsorption, the adsorbed P can be desorbed; but chemical precipitation is dominant, the adsorbed P cannot be desorbed [31].

3.11. Application of the La-JE in real water samples

For assessing the practice application of the La-JE, river water, campus lake water and the effluent from sewage treatment plant were employed as the representative samples. The initial P concentrations in the three samples were 0.09, 0.04 and 0.2 mg·P/L, respectively. Their pH values were in range of 7.35 to 7.68. For every sample, after spiked 0.5 and 1 mg/L of phosphate solution, 2 g/L of La-JE was dispersed in the samples and shaken for 4 h at 25°C according to the above-mentioned method. Finally, all of the effluents displayed a lower phosphate concentrations than 0.02 mg/L which was regarded as the concentration boundary of phosphorus causing to eutrophication [38]. This meant that the La-JE had good potential for advanced dephosphorization of sewage treatment plant and natural waterbody remediation.

3.12. Adsorption mechanism of phosphate on the La-JE

To explore the adsorption mechanism of phosphate on the La-JE, the P-loaded La-JE was analyzed by SEM, XRD and FTIR. From Fig. 2e and f, it can be seen that a lot of amorphous particles appeared on the surface and the gap of the JE fibers, indicating that the phosphate in the solution had entered the La-JE and reacted with the loaded $La(OH)_3$. However, the 3D structure and the coated cellulose film were not damaged, demonstrating that the structure of the La-JE had good stability. From the XRD pattern of P-loaded La-JE (Fig. 3a), the diffraction peaks of $La(OH)_3$ displayed an obvious decrease after adsorbing phosphate. The peaks belonging to $LaPO_4$ were found at 19.8°, 27.2°, 28.6°, 31° and 42.0° [20], demonstrating that phosphate reacted with $La(OH)_3$ and formed $LaPO_4$.

In the FTIR spectrum of the P-loaded La-JE, the adsorption peaks of $La(OH)_3$ disappeared while the bending vibration of O–P–O in PO_4^{3-} was found at 615 and 540 cm^{-1} [39]. The asymmetric stretching vibration of P–O at 1,055 cm^{-1} overlapped with the C–OH deformation vibration and/or C–O stretching vibration in cellulose. These further proved that the reaction between the $La(OH)_3$ and phosphate had happened.

Based on the above results, the removal mechanism of phosphate by the La-JE could be involved in ligand exchange and surface precipitation. For the former, the negatively charged phosphate species exchanged with the hydroxyl

Table 4
Thermodynamic parameters of phosphate adsorption on the La-JE

ΔG (kJ/mol)			ΔS (J/(mol·K))	ΔH (kJ/mol)
25°C	35°C	45°C		
–18.08	–19.38	–21.97	193.28	39.74

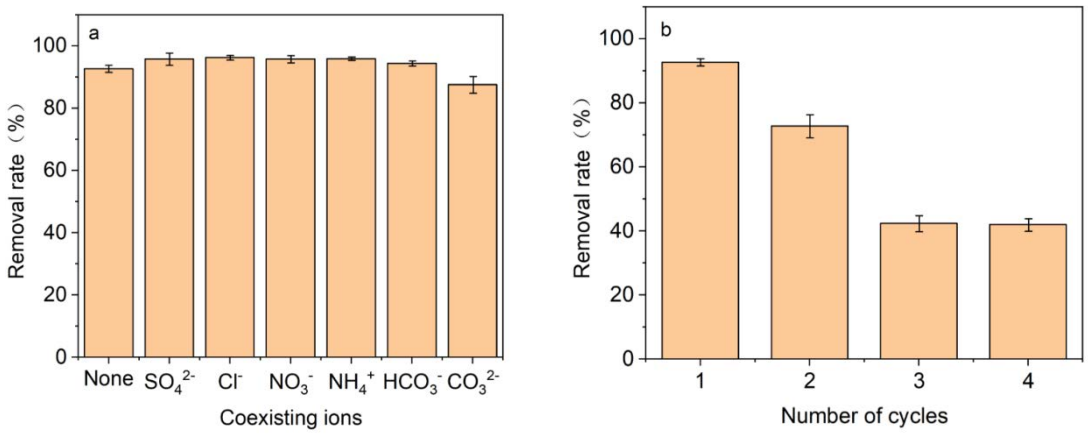

Fig. 7. Influence of co-existing ions on phosphate removal (a) and the reusability of the La-JE (b).

groups of $La(OH)_3$, releasing –OH to the solution. For the latter, it was attributed that phosphate reacted with $La(OH)_3$ followed with the formation of $LaPO_4$ and the release of –OH. This can be further confirmed by the pH change of the reaction medium. According to the results shown in Fig. 2a, it was clear that the final pH values after adsorption gave an increase with the initial pH varying from 2 to 8.

4. Conclusion

$La(OH)_3$-loaded *Juncus effusus* (La-JE) was prepared via an *in-situ* precipitation followed with wrapping a layer of cellulose film. It entirely retained the 3D structure of the JE, which reduced the agglomerate of the active species and was easily separated from aqueous solution. Meanwhile, the introduction of the cellulose film avoided the leakage of La-containing species. According to XRD analysis, the La-containing species loaded on the JE was conformed to be $La(OH)_3$. The optimal pH was found to be 6. The removal rate of phosphate was positively correlated with adsorption time, La-JE dosage and reaction temperature, and negatively correlated with phosphate concentration. The adsorption process complied with pseudo-second-order kinetic model and was better fitted by Freundlich model. The calculated maximum adsorption capacities were 22.75, 23.21 and 23.60 mg·P/g at 25°C, 35°C and 45°C, respectively. Coexisting ions including SO_4^{2-}, Cl^-, NO_3^-, NH_4^+, HCO_3^- and CO_3^{2-} only caused efficiency losses of ±4% for phosphate removal, suggesting that the La-JE had good anti-interference ability. After 4 cycles of adsorption–desorption, the removal rate of phosphate reduced from 93.48% to 43.35%, indicating that phosphate removal on the La-JE was involved in multiple mechanisms. For the chosen water samples, all of the effluents displayed a lower phosphate concentrations than 0.02 mg/L after treatment.

Statements and declarations

No potential conflict of interest was reported by the author(s).

Acknowledgments

This work was financially supported by Science & Technology Program of Sichuan Province (2022YFS0503, 2021YFS0284) and Chengdu Science & Technology Program (2022-YF05-00253-SN).

References

[1] C. Liu, M.Y. Zhang, G. Pan, L. Lundehøj, U.G. Nielsen, Y. Shi, H.C.B. Hansen, Phosphate capture by ultrathin MgAl layered double hydroxide nanoparticles, Appl. Clay Sci., 177 (2019) 82–90.
[2] H.K. Hudnell, C. Jones, B. Labisi, V. Lucero, D.R. Hill, J. Eilers, Freshwater harmful algal bloom (FHAB) suppression with solar powered circulation (SPC), Harmful Algae, 9 (2010) 208–217.
[3] Y. Yao, B. Gao, J.J. Chen, L.Y. Yang, Engineered biochar reclaiming phosphate from aqueous solutions: mechanisms and potential application as a slow-release fertilizer, Environ. Sci. Technol., 47 (2013) 8700–8708.
[4] M.A. Zahed, S. Salehi, Y. Tabari, H. Farraji, S. Ataei-Kachooei, A.A. Zinatizadeh, N. Kamali, M. Mahjouri, Phosphorus removal and recovery: state of the science and challenges. Environ. Sci. Pollut. Res., 29 (2022) 58561–58589.
[5] P. Mullen, K. Venkiteshwaran, D.H. Zitomer, B.K. Mayer, Ion exchange nutrient recovery from anaerobic membrane bioreactor permeate, Water Environ. Res., 91 (2019) 606–615.
[6] D. Dolar, K. Košutić, B. Vučić, RO/NF treatment of wastewater from fertilizer factory – removal of fluoride and phosphate, Desalination, 265 (2011) 237–241.
[7] T. Liu, S.R. Zheng, L.Y. Yang, Magnetic zirconium-based metal–organic frameworks for selective phosphate adsorption from water, J. Colloid Interface Sci., 552 (2019) 134–141.
[8] I.W. Almanassra, V. Kochkodan, G. Mckay, M.A. Atieh, T. Al-Ansari, Review of phosphate removal from water by carbonaceous sorbents, J. Environ. Manage., 287 (2021) 112245, doi: 10.1016/j.jenvman.2021.112245.
[9] R.T. Liu, L.N. Chi, X.Z. Wang, Y.M. Sui, Y. Wang, H. Arandiyan, Review of metal (hydr)oxide and other adsorptive materials for phosphate removal from water, J. Environ. Chem. Eng., 6 (2018) 5269–5286.
[10] F. Zhu, H.J. Lu, Y.H. Lu, Effective solid phase extraction for the enrichment of p-nitrophenol in water using microwave-assisted synthesized fly ash@p-nitrophenol surface molecular imprinted polymer, J. Mater. Sci., 58 (2023) 4399–4415.
[11] N. Parasana, M.N. Shah, A. Unnarkat, Recent advances in developing innovative sorbents for phosphorus removal-perspective and opportunities, Environ. Sci. Pollut. Res., 29 (2022) 38985–39016.
[12] M.X. Li, J.Y. Liu, Y.F. Xu, G.R. Qian, Phosphate adsorption on metal oxides and metal hydroxides: a comparative review, Environ. Rev., 24 (2016) 319–332.
[13] J.W. Lin, B.H. Jiang, Y.H. Zhan, Effect of pre-treatment of bentonite with sodium and calcium ions on phosphate adsorption onto zirconium-modified bentonite, J. Environ. Manage., 217 (2018) 183–195.
[14] N. Mehrabi, M. Soleimani, H. Sharififard, M.M. Yeganeh, Optimization of phosphate removal from drinking water with activated carbon using response surface methodology (RSM), Desal. Water Treat., 57 (2016) 15613–15618.
[15] L. Tao, S.R. Zheng, L.Y. Yang, Magnetic zirconium-based metal–organic frameworks for selective phosphate adsorption from water, J. Colloid Interface Sci., 553 (2019) 134–141.
[16] Q.Q. He, H.J. Zhao, Z.D. Teng, Y. Wang, M. Li, M.R. Hoffmann, Phosphate removal and recovery by lanthanum-based adsorbents: a review for current advances. Chemosphere, 303 (2022) 134987, doi: 10.1016/j.chemosphere.2022.134987.
[17] F. Haghseresht, S. Wang, D.D. Do, A novel lanthanum-modified bentonite, Phoslock, for phosphate removal from wastewaters, Appl. Clay Sci., 46 (2009) 369–375.
[18] J. Xie, Z. Wang, S.Y. Lu, D.Y. Wu, Z.J. Zhang, H.N. Kong, Removal and recovery of phosphate from water by lanthanum hydroxide materials, Chem. Eng. J., 254 (2014) 163–170.
[19] L. Chen, F. Liu, Y. Wu, L.M. Zhao, Y.Z. Li, X. Zhang, J.S. Qian, *In-situ* formation of $La(OH)_3$-poly(vinylidene fluoride) composite filtration membrane with superior phosphate removal properties, Chem. Eng. J., 347 (2018) 695–702.
[20] S.L. Zhang, T. Lin, W. Li, M.L. Li, K. Su, J.M. Chen, H.W. Yang Lanthanum-loaded peanut shell biochar prepared via one-step pyrolysis method for phosphorus removal and immobilization, Environ. Technol., 44 (2023) 1169–1178.
[21] S.Y. Li, X.F. Huang, J. Liu, L.J. Lu, K.M. Peng, R. Bhattarai, PVA/PEI crosslinked electrospun nanofibers with embedded $La(OH)_3$ nanorod for selective adsorption of high flux low concentration phosphorus, J. Hazard. Mater., 384 (2020) 121457, doi: 10.1016/j.jhazmat.2019.121457.
[22] B.L. Wu, L.P. Fang, J.D. Fortner, X.H. Guan, I.M.C. Lo, Highly efficient and selective phosphate removal from wastewater by magnetically recoverable $La(OH)_3/Fe_3O_4$ nanocomposites, Water Res., 126 (2017) 179–188.
[23] S.J. Zhou, L.J. Xia, K. Zhang, Z. Fu, Y.L. Wang, Q. Zhang, L.S. Zhai, Y.S. Mao, W.L. Xu, Titanium dioxide decorated natural cellulosic *Juncus effusus* fiber for highly efficient photodegradation towards dyes, Carbohydr. Polym., 232 (2020) 115830, doi: 10.1016/j.carbpol.2020.115830.

[24] S.L. Zhang, W. Li, M.L. Li, T. Lin, K. Su, H.W. Yang, J.M. Chen, Efficient removal and detoxification of Cr(VI) by PEI-modified *Juncus effusus* with a natural 3D network structure, Sep. Purif. Technol., 297 (2022) 121543, doi: 10.1016/j.seppur.2022.121543.
[25] L. Zhang, Q. Zhou, J.Y. Liu, N. Chang, L.H. Wan, J.H. Chen, Phosphate adsorption on lanthanum hydroxide-doped activated carbon fiber, Chem. Eng. J., 185 (2012) 160–167.
[26] M. Mousavi-Kamazani, S. Alizadeh, F. Ansari, M. Salavati-Niasari, A controllable hydrothermal method to prepare $La(OH)_3$ nanorods using new precursors, J. Rare Earths, 33 (2015) 425–431.
[27] J.D. Zhang, Z.M. Shen, W.P. Shan, Z.J. Mei, W.H. Wang, Adsorption behavior of phosphate on lanthanum(III)-coordinated diamino-functionalized 3D hybrid mesoporous silicates material, J. Hazard. Mater., 186 (2011) 76–83.
[28] Q. Tang, C.H. Shi, W.M. Shi, X.L. Huang, Y.Y. Ye, W. Jiang, J.X. Kang, D.Q. Liu, Y.Z. Ren, D.S. Li, Preferable phosphate removal by nano-La(III) hydroxides modified mesoporous rice husk biochars: role of the host pore structure and point of zero charge, Sci. Total Environ., 662 (2019) 511–520.
[29] L. Chen, Y.Z. Li, Y.B. Sun, Y. Chen, J.S. Qian, $La(OH)_3$ loaded magnetic mesoporous nanospheres with highly efficient phosphate removal properties and superior pH stability, Chem. Eng. J., 360 (2019) 342–348.
[30] W.Y. Huang, Y. Zhu, J.P. Tang, X. Yu, X.L. Wang, D. Li, Y.M. Zhang, Lanthanum-doped ordered mesoporous hollow silica spheres as novel adsorbents for efficient phosphate removal, J. Mater. Chem. A, 2 (2014) 8839–8848.
[31] N. Chen, C.P. Feng, Z.Y. Zhang, R.P. Liu, Y. Gao, M. Li, N. Sugiura, Preparation and characterization of lanthanum(III) loaded granular ceramic for phosphorus adsorption from aqueous solution, J. Taiwan Inst. Chem. Eng., 43 (2012) 783–789.
[32] A.J. Zhou, C. Zhu, W.W. Chen, J. Wan, T. Tao, T.C. Zhang, P.C. Xie, Phosphorus recovery from water by lanthanum hydroxide embedded interpenetrating network poly(vinyl alcohol)/sodium alginate hydrogel beads, Colloids Surf., A, 554 (2018) 237–244.
[33] Y. Zuo, X.N. Fu, Y. Chen, G.R. Cui, M. Liu, Phosphorus removal from wastewater using a lanthanum oxide-loaded ceramic adsorbent, Adsorption, 22 (2016) 1091–1098.
[34] H.Y. Fu, Y.X. Yang, R.L. Zhu, J. Liu, M. Usman, Q.Z. Chen, H.P. He, Superior adsorption of phosphate by ferrihydrite-coated and lanthanum-decorated magnetite, J. Colloid Interface Sci., 530 (2018) 704–713.
[35] P. Koilraj, K. Sasaki, Selective removal of phosphate using La-porous carbon composites from aqueous solutions: batch and column studies, Chem. Eng. J., 317 (2017) 1059–1068.
[36] Y.M. Huang, X.Q. Lee, M. Grattieri, M.W. Yuan, R. Cai, F.C. Macazo, S.D. Minteer, Modified biochar for phosphate adsorption in environmentally relevant conditions, Chem. Eng. J., 380 (2020) 122375, doi: 10.1016/j.cej.2019.122375.
[37] Y. Yao, B. Gao, J.J. Chen, L.Y. Yang, Engineered biochar reclaiming phosphate from aqueous solutions: mechanisms and potential application as a slow-release fertilizer, Environ. Sci. Technol., 47 (2013) 8700–8708.
[38] L. Li, W.G. Jiang, H.H. Pan, R. Xu, Y.X. Tang, J.Z. Ming, Z.D. Xu, R.K. Tang, Improved luminescence of lanthanide(III)-doped nanophosphors by linear aggregation, J. Phys. Chem. C, 111 (2008) 4111–4115.